Ground Penetrating Radar Slice Reconstruction for Embedded Object in Media with Target Follow

QEETHARA KADHIM AL-SHAYEA
MIS Department
Al Zaytoonah University of Jordan
Amman Jordan
kit_alshayeh@yahoo.com

ITEDAL S. H. BAHIA
MIS Department
Al Zaytoonah University of Jordan
Amman Jordan
Itedal_bahia70@yahoo.com

Abstract: - The detection of embedded object from ground penetrating radar GPR imagery is our goal. The GPR image is a cross sectional slices. The embedded objects are metal and/or plastic type. In many fields demand for visualizing objects scanned as cross sectional slices is growing. This research has many real world applications, such as robotic environments, medicine, remote sensing, inspection of industrial parts and geology. An even better way is to visualize the underground object by reconstruction a three-dimensional model of those objects from the slices. Objects here are stable underground while, camera is moving. The task of object track in a cross sectional slices consists of two parts: first gather information on changes between succeeding slices (object detection), and second process this information appropriately to obtain the track of an object. If the object is like cable or pipe. The proposed method starts with two dimensional 2D image preprocessing for each slice. The preprocessing involves multispectral to gray conversion, contrast enhancement, segmenting, thresholding and denoising to modify each 2D image slice individually. Preprocessing algorithms involved in this paper are chosen appropriately to have image without noise, with object detected and with object eliminated. After a preprocessing step the proposed algorithm for object detection starts with objects contour finding in each slice, 2D objects transparency and transformation. The last step is the proposed interpolation technique to build the successive slices until the spaces is filled to find out the embedded object.

Key-Words: - Object Detection, Object Recognition, Ground Penetrating Radar (GPR), Volume Reconstruction, Interpolation, Image Processing, Target Follow.

1 Introduction

GPR is one of nondestructive methods for physical detection, which utilizes similar principles to the reflection seismic method. Compared with the reflection seismic method, the GPR method might provide high-resolution images of characterized stratigraphy because it propagates a pulse of electromagnetic _EM_ energy, with a high frequency ranging from 10 MHz to 1 GHz, through the subsurface. A pulse-mode GPR system was operated in such a way that a high frequency and short pulse EM wave was transmitted into the earth and reflected radar pulse was received using one or more antennas on the ground [1]. GPR deliver vertical two dimensional 2D images slice of the ground

Wong and Cipolla [2] choose the volume intersection approach due to its ability to describe objects with more complex topologies (e.g., object with holes). Based on Szeliski, an algorithm for generating an octree using profiles from multiple views is developed. The main difference between the work presented by Szeliski and the technique developed in [3] is that instead of using a background subtraction technique as described by Szeliski, the object / backtracking binary images are computed directly from the B-spline snakes which are used to extract and represent the profiles during motion estimation.

Marabin, Sorzano, Matej, Fernadez, Carazo, and Herman [3] propose an iterative method for performing 3D reconstruction of 2D crystals in real space.

Dell'Acqua, Sarti, Tubaro and Zanzi [4] propose a semi-automatic approach to the detection of linear scattering objects in geo-radar data sets, based on the 3D radon transform. The method that we propose is iterative, as each detected object is removed from the data set before the next iteration, in order to avoid mutual interference or masking.

Ristic, Petrovacki and Govedarica [5] present a new method to simultaneously estimate cylindrical object radius (R) and electromagnetic (EM) wave propagation velocity (v) from ground penetrating radar (GPR) data.

Fruehauf, Heilig ,Schneebeli ,Fellin and Scherzer [6] studied a two-step algorithm to locate avalanche

victims in real time. The algorithm was validated using realistic test arrangements and conditions using an aerial tramway. The distance dependence the reflection energy with increased flight heights, the coherence between the use of more antennas and the detectable range, and the reflection images of different avalanche victims were measured. The algorithm detected an object for each investigated case, where the reflection energy of the scans was higher than for the scans of pure snow. Airborne GPR has a large potential become a rapid search method in dry snow avalanches. However, a fully operational version still requires substantial improvements in hardware and software.

Jeng , Li, Chen and Chien [7] are designed two filters by adopting adaptive algorithms, the optimum 2D median filter, (a 2D median filter with an optimum window size), and the 2D adaptive Wiener filter (a real time optimal filter renovated from the conventional Wiener filter technology) to investigate the advantages of using adaptive filters in processing ultra-shallow seismic and ground-penetrating radar data.

Mohamed K., Abdullah, R. and Raseed M. [8] have presented an analytical and experimental study for extracting the Doppler signature in FSR for ground target detection. Target signal under the influenced of high clutter has been successfully detected using the proposed method. The detection using Hilbert Transform is only applicable if the target's signal has significant difference from the average noise level. But, detection using Wavelet de-noising is more robust against any clutter and noise. The results again confirmed the feasibility of FSR to be employed as an automatic ground target detection system.

Pasolli, Melgani and Donelli [9] propose a novel pattern-recognition system to identify and classify buried objects from ground-penetrating radar (GPR) imagery. The entire process is subdivided into four steps. After a preprocessing step, the GPR image is thresholded to put under light the regions containing potential objects. The third step of the system consists of automatically detecting the objects in the obtained binary image by means of a search of linear/hyperbolic patterns formulated within a genetic optimization framework.

Negahdaripour, Sekkati and Pirsiavash [10] propose methods for system calibration and 3D scene reconstruction by maximum likelihood estimation from noisy image measurements. The recursive 3D reconstruction method utilized as initial condition a closed form solution that integrates the advantages of two other closed form solution.

Yang, Wang, Liu, Tang and Chen [11] present a novel method for the 3D reconstruction of coronary arteries from two uncalibrated monoplane angiographic images. A non-linear optimization method is

developed which takes the influence of the table movement into account for the refinement of 3D structure of vessel skeletons.

Shihab and Al-Nuaimy [12] present an automatic target-detection and localization system based on unsupervised neural network classifier along with some image processing techniques to extract useful data representing targets (such as pipes, tanks, reinforcement bars, and voids) and discard undesirable data (such as noise and clutter). The neural classifier is capable of returning 3-dimensional images outlining regions of extended targets and pinpointing the location of localized targets such as mines and pipes. This classifier was applied to a variety of GPR data sets gathered from a number of sites, and it achieved rapid and accurate results.

H. Parsiani, E. Mattei [13] have presented open field soil moisture determination based on the MCFD/NN algorithm is further explored with data obtained from a four-day campaign at the University of Puerto Rico Mayagüez Campus' baseball field.

L. Yun, W. Seng, B. Yong and L. Ping [14] present an architecture which enables 3D heart model visualization tasks to be performed efficiently in collaboration environment.

S. Rashwan, M. Ismail and S. Fouad [15] have proposed an approach based on possibility theory. The approach is based on computing the correlation among different images taken at different times to study the change of the environment and use it as a parameter in four T-Norm Correlation-Dependent fusion techniques to handle the problem of high correlation by introducing the correlation parameter in the fusion process.

2 Multidimensional image Preprocessing

The preprocessing algorithms, techniques, and operators are used to perform initial processing that makes the primary data reduction and analysis task easier. They include operations related to extracting regions of interest, performing basic algebraic operations on images and enhancing specific image features [16].

The goal of image enhancement is to prepare raster images for further processing or for display by removing noise or enhancing contrast. It is usually performed by applying some functions to the image, so that the input image f is transformed into an output image g using a filter functional T [17].

Digital volumetric image are stacks of 2D image slices. We can think of these slices as serial cross–sections through a scene depicting objects in a digitized 3D world. The set of addresses is sometimes

referred to as the image lattice. More precisely, the image lattice is the set:

$\{(s,r,c)| \ 0 \le s < nslices, \ 0 \le r < nrows, \ 0 \le n < ncolumns\}$
where nslices, nrows, ncolums denote the number of slices, rows and columns [17]. Fig. 1 illustrates a stack of slices.
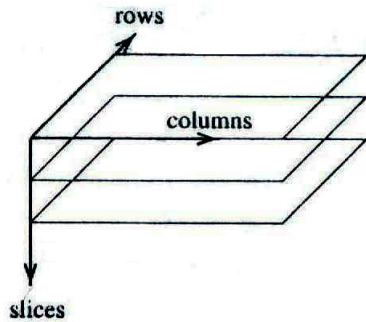

Fig. 1 A stack of slices.

3 The Proposed image Preprocessing

Some image data collecting techniques such as Ground Penetrating Radar image (GPR) generate a series of cross sectional images from which 3D object geometry and density features have to be extracted and reconstructed. Our data are 2D slices GPR images of underground viewed in sagittal direction as in Fig. 2.
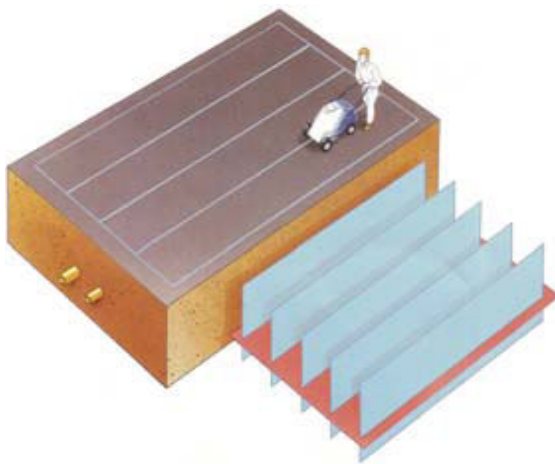
Fig. 2

The microwave images of the objects embedded in the ground are included the soil effected and unwanted objects in addition to the wanted objects. However some preprocessing can be used to distinguish the required objects in the 2D images. Fig. 3 shows a GPR image slice 1. Fig. 4 shows a GPR image slice 2.
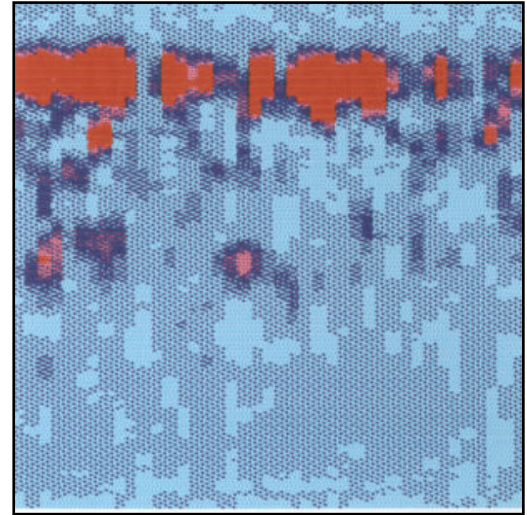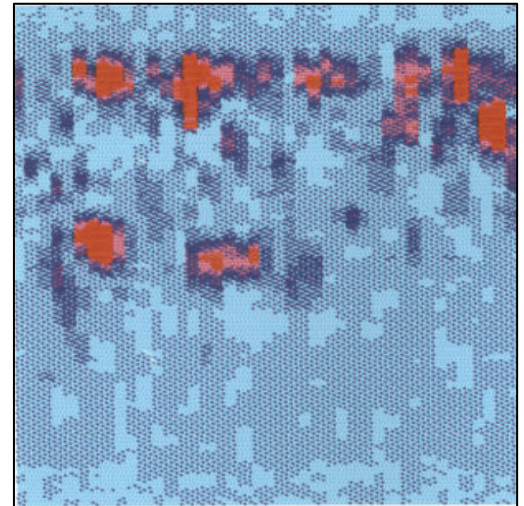

Fig. 3 GPR slice 1

Fig. 4 GPR slice 2

Image preprocessing is used to have appropriate slices. The resultant slices will be taken to reconstruct 3D image. Fig. 5 demonstrates the flowchart for image preprocessing proposed.

After the slice is read, the proposed conversion method to multispectral slice is done. The proposed conversion depends on display the metallic and plastic objects in the image. Since the image size must be compatible with the real world, image resize is chosen to be the next preprocessing stage. Then draw the histogram for each slice to study it. From studying the histogram of images, as shown in Fig. 6 it is obvious that the contrast is very low. So, to enhance the contrast of an image there are more than one way. Since images are better to be enhanced using histogram equalization compared with high pass filter as practical experiment proved, it is chosen.
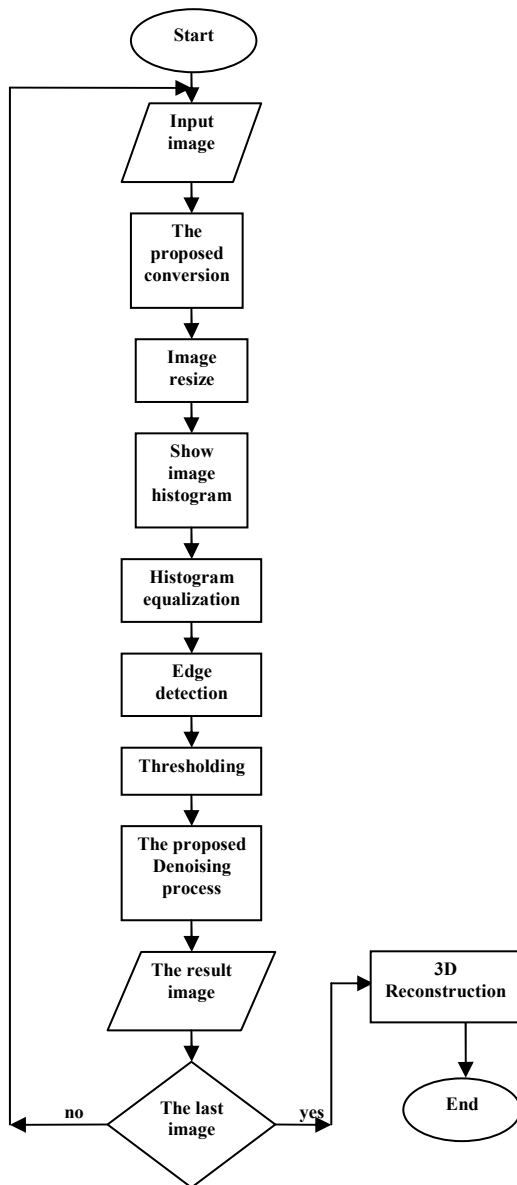
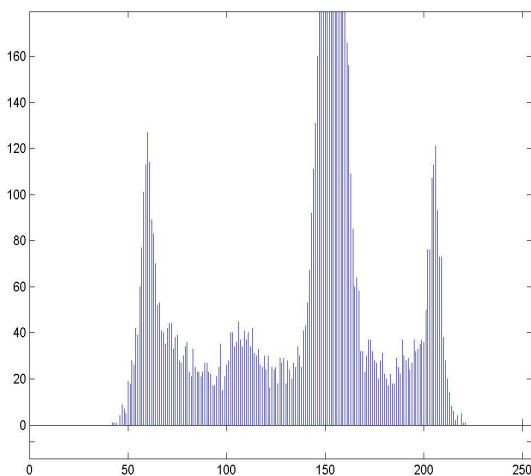Fig. 5 Flowchart of the proposed image preprocessing

Fig. 6 GPR slice 1 histogram

Because of its capability to detect edge in all directions, Kirsch compass mask is preferred. Thresholding is the best process to be used after edge detection. In each slice the adjacent pixels less than five are eliminated. In the modified denoising process, a median filter is developed in such a way as to eliminate adjacent pixels less than five.

3.1 The Proposed Denoising Algorithm

Median filter is used to eliminate noise of an impulsive nature. Suppose that the diameter of each embedded object is equal to 12.5 centimeters. The following computations are used to compute the number of adjacent pixels to be eliminated.

The width of each slice / number of row in each slice =
$$400 / 128 = 3.125 \text{ centimeters}$$
Number of pixels to be eliminated = diameter of each object / 3.125

$$= 10 / 3.125$$
$$= 4 \text{ pixels}$$

So, the purpose here is to eliminate adjacent pixels less than or equal to four pixels. Since median filter does not satisfy this purpose a modified denoising algorithm is proposed to eliminate the noises which appear in the threshold images. The steps of the proposed method are as follows:

1. Apply median filter using 3x3 convolution masks.
2. Check the objects in the image; say for example 6 adjacent pixels.
3. If the number of adjacent pixels less than or equal 4 in 3x3 windows, then delete these pixels.

Fig. 7 and Fig. 8 show the result of applying the proposed algorithm to proposed conversion method on slice 1 and slice 2. The line in the resultant image represents the surface earth. To specify the depth of the object from the earth surface the distance between this line and the object must be determined.
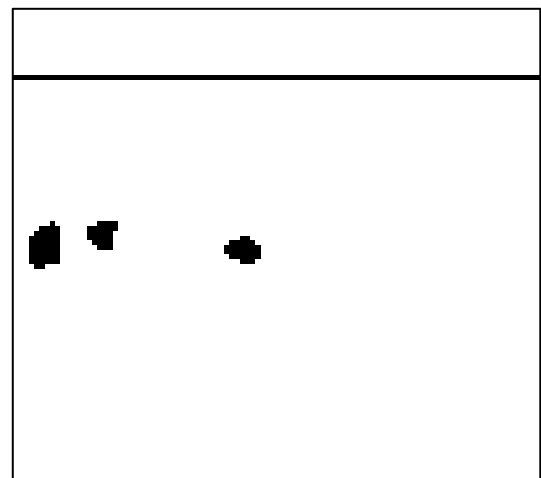

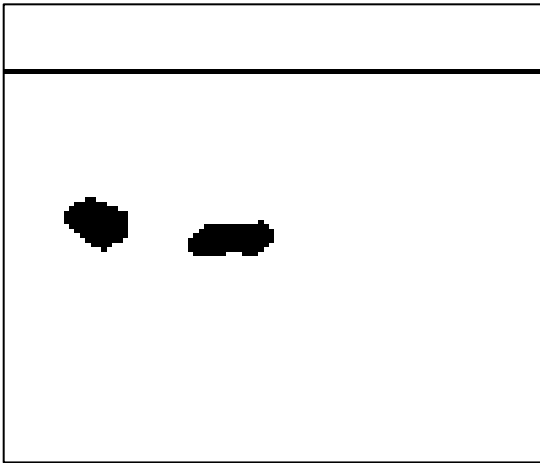Fig. 7 slice 1 after denoising process

Fig. 8 slice 2 after denoising process

4 The proposed Methodology

Algorithm for a visible volume reconstruction from 2D image slices is proposed. This algorithm consists of contour generation, objects transparency, image translation and rotation.

The volume visualization means a generation of comprehensible representations from 3D scalar fields for a variety of application fields. Currently every GPR data set consists of an arbitrary number of slice images which are scanned at equidistant locations. Therefore, all slices together represent a volume if they are arranged according to their spatial positions. Therefore, every slice forms a matrix of MxN where M=128,256,… N=128,256,… and in some cases even 1024^2 sample points [18]. However, the visible volume reconstruction forms a matrix of MxNxL.

The proposed method of the volume reconstruction will be described to reconstruct the 3D image from 2Dslices. Schematic diagram of image data collecting is shown in Fig. 9.
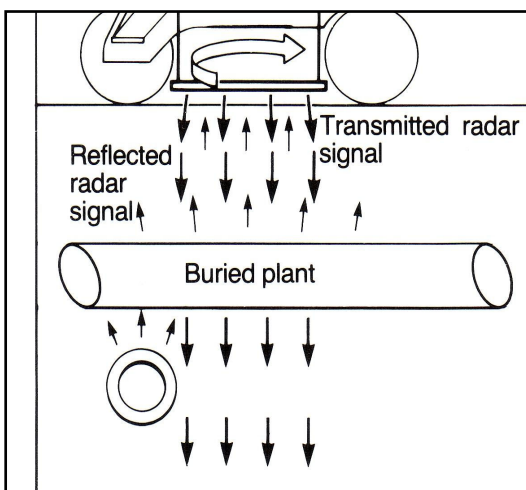

Fig. 9 Schematic diagram of image data collecting.

An algorithm for the proposed methodology is described as follows:
1- Input the binary level image I_{inp} of size nrxnc. Also, input the number of images nb.
2- Put the data image of size jxi one after the other in a stack.
3- for j= 0,1,2,…,nr
    for i= 0,1,2,…,nc
    for k= 0,1,2,…,nb
Indicate the image with k_{nb}

4- for j= 0,1,2,…,nr
    for i= 0,1,2,…,nc
    for k= 0,1,2,…,nb
Find contour for each object in the image.
5- for j= 0,1,2,…,nr
    for i= 0,1,2,…,nc
    for k= 0,1,2,…,nb
Translate the image with the number of spaces between them to the x-axis and y-axis.
6- for j= 0,1,2,…,nr
    for i= 0,1,2,…,nc
    for k= 0,1,2,…,nb
Rotate the image by an angel θ_0.

7- Find the interpolation between two images.
8- Insert the interpolated images between the original data.

4.1 Contour Generators

If the number of quantization levels is not sufficient, a phenomenon called contouring becomes visible.
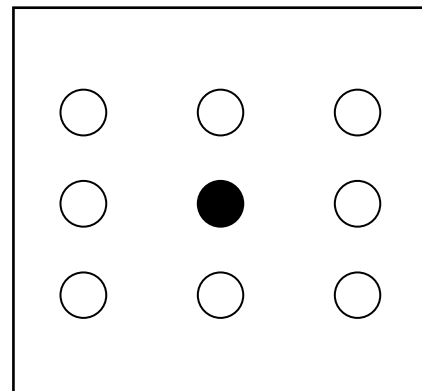Fig. 10 shows the 8-connected neighbors.

Fig. 10 8-connected neighbors.

Tracing of closed boundaries in images is as follows:
1- Scan the image.
2- If object is found label it by object A.
3- Start inside object A.
4- Turn left and step to next pixel if in region A, otherwise turn right and step to next pixel.
5- Continue until arrive at starting point.

The contour is the first step in reconstruction process. The contours are found by scanning the whole image for values other than 255 and if this pixel has a neighbor which is a background 255 then it is recorded as contour pixel, otherwise it is not contour pixel. When we look for neighboring background pixels, the algorithm examines the up, down, right, left, upper right, upper left, down right, and down left pixels only so that the produced contour is 8-connected with the background.

4.2 3D Image Transformation

The ability to represent or display a 3D object is fundamental to the understanding of the shape of that object. Furthermore, the ability to rotate, translate, and project views of that object is also, in many cases, fundamental to the understanding of its shape [19].
3D translation matrix is:

$$[T] = \begin{bmatrix} 1 & 0 & 0 & 0 \\ 0 & 1 & 0 & 0 \\ 0 & 0 & 1 & 0 \\ h & k & l & 1 \end{bmatrix}$$

Depending on the distances between successive slices the translated homogeneous coordinates are obtained by writing

$$[x' \quad y' \quad z' \quad h] = [x \quad y \quad z \quad 1] \begin{bmatrix} 1 & 0 & 0 & 0 \\ 0 & 1 & 0 & 0 \\ 0 & 0 & 1 & 0 \\ l & m & n & 1 \end{bmatrix}$$

$$[x' \quad y' \quad z' \quad m] = [(x+l)(y+m)(z+n)1]$$

so,

$$x' = x + l$$
$$y' = y + m$$
$$z' = z + n$$

Fig. 11 shows the translation to two successive slices without transparency, while l=6, m=6 and n=1. This yield

$$x' = x + 6$$
$$y' = y + 6$$
$$z' = z + 1$$

It is obvious that the last slice displayed on the screen is hiding the first one.
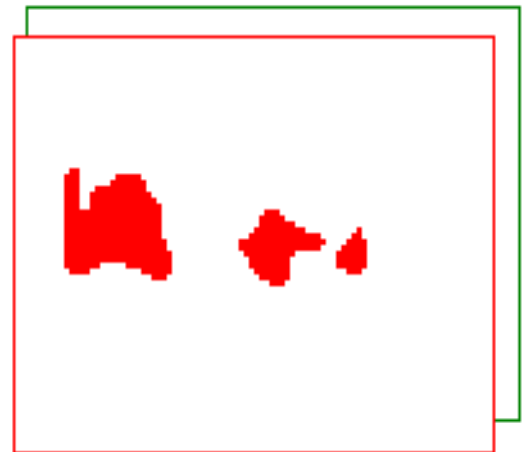

Fig. 11 Translation without transparency.

4.3 Object Transparency

When an image is displayed on the screen and the next image is displayed in sharing location with the previous image on the screen, the objects in the next image will hide the first one. This means that sharing locations between images are dedicated to the last one with hiding of the others. To overcome this situation a new method is presented. This method is the transparency which is to be after contour process. Therefore, transparency method is done to display the sharing pixels between slices. The result of transparent method between two slices is shown in Fig. 12. By comparing between translation with transparency as shown in Fig. 12 and translation without transparency as shown in Fig. 11, it is clear that volumetric is not possible to make without transparency.
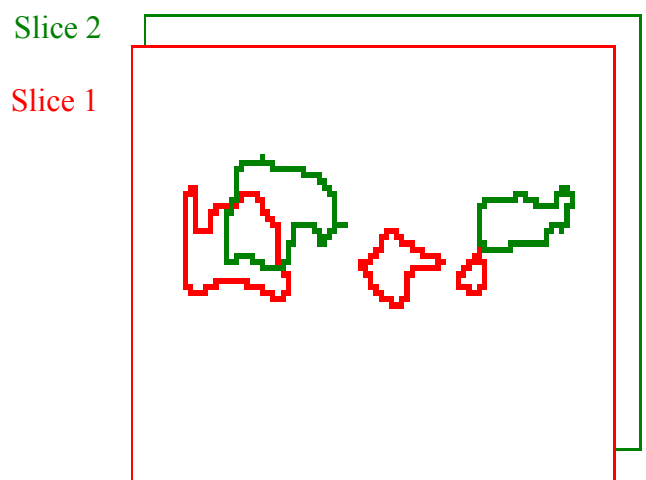

Fig. 12 Transparency between two slices after translation.

Before considering 3D about an arbitrary axis, we examine rotation about each of the coordinate axes. For rotation about the x-axis, the x coordinates of the position vectors do not change. In effect, the rotation occurs in planes perpendicular to the x-axis. Similarly, rotation about the y-and z-axes occurs in planes perpendicular to the y- and z-axes, respectively.

The trigonometric ratios (sine and cosine) of the angle of rotation are used. When we rotate a point about the x-axis, through an angle θ, its x-coordinate is unaltered. Thus the first row and the first column in this matrix do not involve θ. For rotation about the x-axis the form of the matrix is:

$$\begin{bmatrix} 1 & 0 & 0 & 0 \\ 0 & \cos\theta & \sin\theta & 0 \\ 0 & -\sin\theta & \cos\theta & 0 \\ 0 & 0 & 0 & 1 \end{bmatrix}$$

In a rotation through an angle ψ about the z-axis the z-coordinates of points are unchanged, and so the third row and the third column of the matrix will not involve ψ. A matrix for rotation about the z-axis is:

$$\begin{bmatrix} \cos\Psi & \sin\Psi & 0 & 0 \\ -\sin\Psi & \cos\Psi & 0 & 0 \\ 0 & 0 & 1 & 0 \\ 0 & 0 & 0 & 1 \end{bmatrix}$$

When a point is rotated about the y-axis through an angle Φ, then the y-coordinates are unchanged, and so it is the second row and the second column of the matrix that do not involve Φ. There is an important difference to be noted in the pattern of the signs of the 'sin Φ ' terms in this case: this change is necessary to preserve the right-handed rotation convention. To rotate about the y-axis we have a matrix of this form:

$$\begin{bmatrix} \cos\Phi & 0 & -\sin\Phi & 0 \\ 0 & 1 & 0 & 0 \\ \sin\Phi & 0 & \cos\Phi & 0 \\ 0 & 0 & 0 & 1 \end{bmatrix}$$

4.4 Interpolation Scheme

Image interpolation is an important technique in the field of the 3D reconstruction from cross sectional images. Several different interpolation schemes have been used in the past. The most widely used is the so-called trilinear interpolation scheme. The basic idea of trilinear interpolation scheme is to sum up the values of the eight adjacent voxels, where each of the eight values is weighted according to its distances from the true location. Fig. 13 shows this arrangement [16].
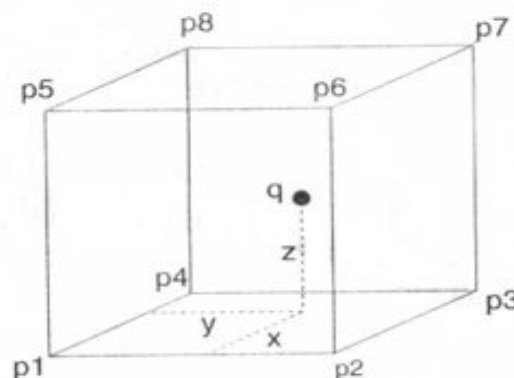

Fig.13 Trilinear Interpolation.

Since the trilinear interpolation not serves the process to reconstruct 3D objects, an idea is proposed. The proposed idea is making the logical AND operation between successive slices then we have the interpolated slice.

The distance between successive slices is calculated. So, all empty spaces should be filled instead of leaving to the viewer's imagination.

5 Object Detection Process

Objects here are stable underground while, camera is moving. The task of object track in a cross sectional slices consists of two parts: first gather information on changes between succeeding slices (object detection), and second process this information appropriately to obtain the track of a object.

In each slice, there are a number of objects which represent the targets. These targets are detected by recognizing the color of object from the background. When the object is recognized, it will be filled with a gray value which differs from other objects in the same slice such that the first object is filled with gray value equal to 147 while, the other with 75 and so on. This process is done to the first slice only. Fig. 14 shows the first slice of real model with its new gray level. From Fig. 14, it is clear that there are three objects in slice 1 and each object has different gray value from the others.

Fig.14 Slice 1 with its new gray value.

Then for the next successive slice, if object is found by recognizing it from its background, an AND operation is proposed between the same locations in successive slices. If the result from AND operation is equal to nonzero then, this object will be filled with the gray value equal to the gray value of the object in the previous successive slice, while, if the result is equal to zero, the object will be filled with different gray value. This process is done until all slices with their objects are detected and filled with gray value. Flowchart for this process is shown in Fig. 15.

A new algorithm of tracking the embedded target is presented. Target detection is the first step in the new tracking algorithm.
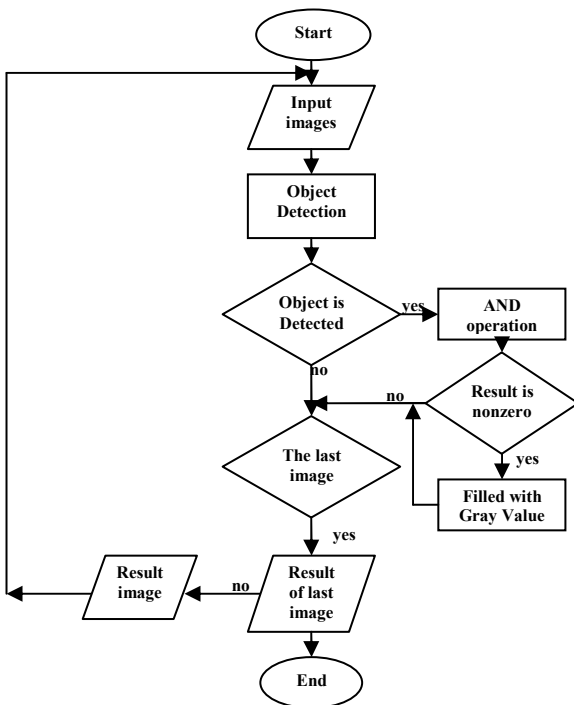

Fig. 15 Flowchart of Target Detection Algorithm.

5.1 The proposed Tracking Algorithm

The proposed algorithm depends on the gray scale value of object. If the objects in successive slices have the same gray scale value, these objects are bordered with the same color to represent the target. Objects that have gray value not equal to any gray value in other slices are bordered with another color.

Since the information provided for following targets is serial cross section, the spaces between them should be interpolated. Usually, the cross sections are not evenly spaced in order to capture the most significant parts of the object; the number of scans is limited to reduce the radiation dose delivered to the object. So it is important to fill the spaces between these slices using interpolation technique.

Since trilinear interpolation not serve the process to reconstruct 3D objects, we propose the idea of making the logical AND operation between successive slices then we have the interpolated slice.

In our images the distance between successive slices is equal to 6 spaces (pixels). So, all empty spaces should be filled instead of leaving to the viewer's imagination. For example, when we have 10 slices then we should fill the spaces between them by 63 slices. The proposed interpolation between slice 1 and slice 2 is shown in Fig. 16. Practically, the images in the resultant slice appear as logical AND operation as shown in Fig. 16. However, it is easer to distinguish the relationship between the same targets in successive slices.

If we have five slices with three spaces between them the slices to be filled between them should be equal to 12 slices.
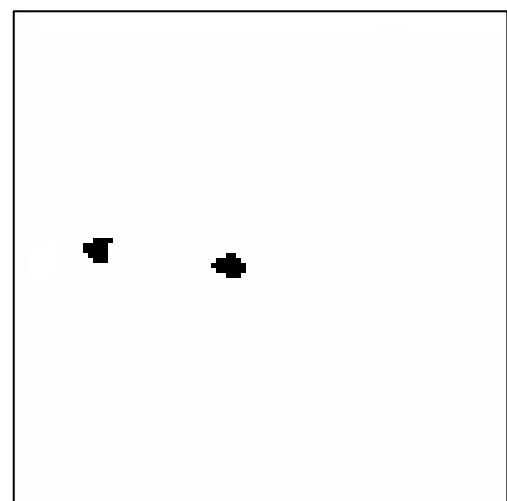

Fig. 16 Trilinear interpolation between slice 1 and 2.

6 Conclusions

This work presents a technique for 3D reconstruction from 2D cross sectional slices. The purpose of this reconstruction is object detection. The input is GPR successive slices. Specific points of interest of the proposed methods are the use of 2D image preprocessing with its technique as robust methods for the automatic determination of effective starting points of the 3D reconstruction algorithm.

The first algorithm is image preprocessing for each slice. The preprocessing involves multispectral to gray conversion, contrast enhancement, segmenting, thresholding and denoising to modify each 2D image slice individually. Preprocessing algorithms proposed in this paper are chosen appropriately to have image without noise, with object detected and with object eliminated.

After preprocessing a proposed 3D reconstruction methodology is presented. The first stage in the proposed methodology is contour finding. The second stage is to cumulate the data images in stack. It is note from practical implantation that the intersection of two contour generators from two distinct view points generates a point that is visible in both images as a fixed point. Object transparency is the third stage that makes the intersected slices visible. Then translate the images depending on the distances between slices. The translation is to x-axis and y-axis. Rotation will be by an angel θ_0 is the last process in our proposed method. The modified interpolation is needed to improve the proposed volume reconstructing objects from serial cross sections.

References

[1] W. Ting-Nien and H. Yi-Chu**,** Detection of Illegal Dump Deposit with GPR: Case Study, Practice Periodical of Hazardous, Toxic & Radioactive Waste Management, Vol.10, No.3, Jul 2006, pp144-149.

[2] K. K. Wong and R. Cipolla, Reconstruction of Sculpture from its Profiles With Unknown Camera Positions, IEEE TRASACTIONS on Image Processing, Vol.13, No.3, March 2004, PP. 381-389.

[3] R. Marabini, C. S. Sorzano, S. Matej, J. J. Fernadez , J. M. Carazo and G. T. Herman, 3D Reconstruction of 2D Crystals in Real Space, IEEE TRANSACTIONS on Image Processing, Vol.13, No.4, Apr 2004, PP. 549-561.

[4] A. Dell'Acqua, A. Sarti, S. Tubaro and L. Zanzi**,** Detection of linear objects in GPR data, Signal Processing, Vol.84, No.4, Apr 2004,pp785-800.

[5] A. V. Ristic, D. Petrovacki and M. A. Govedarica, new method to simultaneously estimate the radius of a cylindrical object and the wave propagation velocity from GPR data, Computers & Geosciences,Vol.35, No.8, Aug 2009, pp1620-1630.

[6] F. Fruehauf, A. Heilig, M. Schneebeli, W. Fellin and O. Scherzer, Experiments and Algorithms to Detect Snow Avalanche Victims Using Airborne Ground-Penetrating Radar, IEEE Transactions on Geoscience & Remote Sensing, Vol.47, No.7, Jul 2009, pp2240-2251.

[7] Y. Jeng, Y. Li, C. Chen and H. Chien, Adaptive filtering of random noise in near-surface seismic and ground-penetrating radar data**,** Journal of Applied Geophysics, Vol.68, No.1, May 2009, p p36-46.

[8] K. Mohamed, R. Abdullah and M Raseed, Detection of Ground Target in Forward Scattering RADAR Using Hubert Transform and Wavelet Technique, International Review of Electrical Engineering (LR.E.E.), Vol.4, No.2, March-April 2009, pp320-326.

[9] E. Pasolli, F. Melgani and M. Donelli, Automatic Analysis of GPR Images: A Pattern-Recognition Approach, IEEE Transactions on Geoscience & Remote Sensing, Vol.47, No.7, Jul 2009, pp. 2206-2217.

[10] S. Negahdaripour, H. Sekkati and H. Pirsiavash, Opti-Acoustic Stereo Imaging: On System Calibration and 3-D Target Reconstruction, IEEE TRANSACTIONS on Image Processing, Vol.18, No.6, June 2009, PP. 1203-1214.

[11] J. Yang, Y. Wang, Y. Liu, S. Tang and W. Chen, Novel Approach for 3-D Reconstruction of Coronary Arteries From Two Uncalibrated Angiographic Images, IEEE TRANSACTIONS on Image Processing, Vol.18, No.7, July 2009, PP. 1563-1572.

[12] S. Shihab, and W. Al-Nuaimy, Image Processing and Neural Network Techniques for Automatic Detection and Interpretation of Ground Penetrating Radar Data, www.wseas.us/e-library/conferences/crete2002/papers/444-717.pdf.

[13] H. Parsiani, E. Mattei, Open field soil moisture measurements with Radar, WSEAS Int. Conf. on REMOTE SENSING, Venice, Italy, Nov 2-4, 2005, pp 61-64.

[14] L. Yun, W. Seng, B. Yong and L. Ping, A Tele collaborative Surgery Framework for 3D Heart Model, 7th WSEAS International Conference on APPLIED COMPUTER SCIENCE, Venice, Italy, November 21-23, 2007, pp 173-177.

[15] S. Rashwan, M. Ismail and S. Fouad, Detection of Buried Landmines using the Possibilistic Correlation-Dependent Fusion Methods, Proceedings of the 6th WSEAS International Conference on Signal Processing, Robotics and Automation, Corfu Island, Greece, February 16-19, 2007, pp 42-47.

[16] S. E. Umbaugh, Computer Vision and Image Processing: A Practical Approach Using CVIPtools,

Prentice Hall PTR, A Simon and Schuster Company, 1998.

[17] G. Lohmann ., Volumetric Image Analysis, John Wiley & Sons Ltd & T. G. Teubner, 1998.

[18] B. Girod , G. Greiner and H. Niemann, Principles of 3D Image Analysis & Synthesis, Kluwer Academic Publishers, 2000.

[19] D. F. Rogers and J A. Adams, Mathematical Elements for Computer Graphics, McGraw-Hill, Inc., 1990.